Limitations of Temporal Resolution in Functional MRI

Seong-Gi Kim, Wolfgang Richter, Kâmil Uğurbil

In fMRI, images can be collected in a very short time; therefore, high temporal resolution is possible in principle. However, the temporal resolution is limited by a blurred intrinsic hemodynamic response and a finite signal-to-noise ratio. To determine the upper limit of temporal resolution in a single area during repeated tasks, motor cortex activity was investigated during visually instructed finger movements. *Without averaging*, a sequence of four single-finger movements with an execution time of approximately 2 s can be resolved when the delay time between consecutive sequences is at least 3 s. The hemodynamic response time is constant for each subject, but not among different subjects. The temporal resolution can be better when the signal from spatially distinct regions is examined. For a series of experiments involving a visually instructed *delayed* cued finger movement task with a well-defined, independently determined, variable delay time, time courses in the motor area are distinct from each other in two experiments if the difference in delay time is as little as 2 s. The activation in the visual area due to the presentation of the task serves here as an internal time reference. By comparing a set of fMRI time courses in multiple distinct areas, serial neural processing may be investigated.

Key words: fMRI; functional mapping; neuro-imaging; serial neural processing.

INTRODUCTION

Understanding brain function requires information not only on the spatial localization of neural activity, but also on its temporal evolution. Currently, spatial information can be obtained in the human brain by using several techniques based on regional cerebral blood flow (rCBF), such as positron emission tomography (PET) (e.g., ref. 1), single photon emission tomography (SPECT) (for a review, see ref. 2), and most recently, functional magnetic resonance imaging (fMRI) (e.g., 3–5). The basis of these techniques, beginning with the experiments of Roy and Sherrington (6), is that rCBF alterations are closely related to neuronal activity. Mapping of brain function with these techniques is usually obtained by creating a *steady state* condition of the brain through continuously repeated tasks and therefore lacks *temporal* information about neural activity. Studies with a temporal resolution of milliseconds can be conducted by electroencephalographic (EEG) and magnetoencephalographic (MEG) methods (e.g., 7, 8), which are based on electric or magnetic activity caused by movements of ions inside and outside of cellular membranes. However, these methods provide poor spatial localization and resolution.

Before the temporal characteristics of neural events are investigated by fMRI, the question of temporal resolution, measured by the interval between temporally separable task-induced fMRI responses, should be addressed. fMRI images can be acquired in tens of milleseconds; for example, on our 4 Tesla MRI system, a two-dimensional image with a size of 64 × 64 pixels can be recorded in 30 ms by using an echo planar imaging (EPI) technique; including a delay for T_2* weighting brings the time for single image acquisition in an fMRI study to approximately 50 ms (9, 10). However, the temporal resolution is limited by a finite signal-to-noise ratio (SNR) combined with a blurred intrinsic hemodynamic response. In an early study, Bandettini *et al.* (11) investigated the BOLD signal responses during alternating finger movement and rest periods at different switching frequencies at 1.5 Tesla. When the switching frequency was 0.062 Hz (i.e., 8.0 s movement and 8.0 s control), the response due to each task period was separable in the time courses. However, the separation could not generally be achieved at a frequency of 0.125 Hz. Hence the temporal resolution, again defined as the time between two separable tasks, for *the same area* was ≥8 s in a single trial (but may be improved by signal averaging). Here we extend these early and preliminary studies of temporal resolution by using a high field MRI system, which provides increased SNR and BOLD effect (12–14), hence allowing us to use *single trials without averaging.*

To address temporal resolution, the reproducibility of the hemodynamic response function must be assessed. Functional location, parameterized by a center-of-mass-like quantity, is typically reproducible, but signal intensity changes and activation volumes may not be reproducible during repeated tasks, not even in the same subject. Many compounding neuropsychological and neurophysiological effects can contribute to the fMRI signal, and, in addition, the hemodynamic response may depend on the vascular architecture (15). To minimize neuropsychological effects, a relatively simple finger movement paradigm was used; actual finger movement times were recorded. To determine the reproducibility and variability of the fMRI signal, we compared hemodynamic responses in the motor area during movements in a single subject and in different subjects.

When hemodynamic responses in two regions occur at different times, the difference may or may not reflect a difference in neuronal events. If the hemodynamic response times in all regions and in all subjects were the same, neuronal activities could be directly inferred from fMRI time courses. The difference between two regions in hemodynamic response time can be measured by using two different stimuli with a temporal offset (16, 17). For example, in studies of the visual cortex, the onset of

MRM 37:631–636 (1997)

From the Center for Magnetic Resonance Research, Department of Radiology, University of Minnesota Medical School, Minneapolis, Minnesota.

Address correspondence to: Seong-Gi Kim, Ph.D., CMRR, University of Minnesota Medical School, 385 E. River Road, Minneapolis, MN 55455.

Received July 11, 1996; revised September 19, 1996; accepted October 9, 1996.

This work was supported by NIH grants RR08079, NS32919 and NS32437, and a Grant-in-Aid from the University of Minnesota.

0740-3194/97 $3.00

the visual stimulus in one hemifield was offset by 500 ms relative to the other hemifield (16). Relative hemodynamic response differences between the hemispheres were found to be similar to the behavioral difference of 500 ms, suggesting that hemodynamic response times in these two regions are identical. However, since the hemodynamic response is closely related to the vascular architecture (15), this may not be true in all regions and in all subjects, and thus differences in fMRI time courses may be simply related to intrinsic hemodynamic response time differences, hampering temporal studies. To examine whether temporal neuronal activities can be deduced from fMRI time courses of multiple regions in the presence of different intrinsic hemodynamic response times, a well-known visuo-motor task, studied extensively in monkeys, was used (e.g., 18). This task consists of visual presentation, delay period, and cued finger movements. According to single neuronal recordings in monkeys, neurons in the primary motor area fire extensively during motor execution, and much less (ca. 14% of neurons involved in motor execution) during the motor preparation period (18). We assumed furthermore that neurons in the visual cortex are activated during the visual presentation. The neuronal activity in the motor area and corresponding hemodynamic response can be temporally shifted relative to the visual area by varying the delay time between visual presentation and motor execution. Differences of fMRI time courses in two areas can then be compared with the delay times, i.e., with known neuronal activities.

In summary, we examined the temporal resolution of fMRI by using tasks involving the motor area. We undertook two different approaches, both using the EPI technique; one measured activation during repeated episodes of movements, and the other measured activation during performance of visually instructed, delayed motor tasks with variable delays. Functional MRI time courses were compared with behavioral data, i.e., finger movements and reaction times.

METHODS

All MRI studies were conducted on a 4 T whole body imaging system with a 1.25 M diameter horizontal bore (Varian, Palo Alto, CA/Siemens, Erlangen, Germany) and a head gradient insert operating at gradient strength of 30 mT/m and a slew rate of 150 T/m/s in all three axes. For RF transmission and detection, a homogeneous birdcage coil was used (19). Manual shimming was performed before the EPI data collection.

Healthy volunteers were studied according to guidelines set forth by the institutional review board of the University of Minnesota; informed consent was obtained from all subjects. The subjects used their dominant hand to perform tasks. While lying in the bore of the magnet, subjects viewed a rear-projection screen on which computer-generated paradigms were displayed. The interval between the visual cue and the corresponding finger movement (i.e., the reaction time; RT) was recorded through a touch pad with a button for each of the four fingers, connected to an IBM personal computer. The finger movement was also recorded independently and continuously by a pressure sensor located at the bottom of the touch pad with a sampling frequency of 100 Hz (20), together with a signal generated by the pulse program at the beginning of each EP image. These behavioral data can be directly compared with fMRI data.

Before each functional imaging study, sagittal and axial anatomic images were acquired with conventional TurboFLASH techniques (21). From these images, slices for functional imaging were identified on the basis of known brain anatomy. Typically, coronal slices containing the calcarine fissure and the central sulcus were chosen for visual and motor areas, respectively. Anatomic T_1-weighted TurboFLASH images were collected in planes identical to the functional imaging slices [echo time (TE) = 3 ms, inversion time (TI) = 1.2 s, and matrix size = 128 × 128 pixels]. In addition, T_1-weighted EPI images with 128 × 128 matrix size were acquired by an interleaved technique (10). Typical parameters here were TI = 1.2 s, TE = 8 ms, field of view (FOV) = 24 × 24 cm^2, and number of segments = 4. The T_1-weighted images provided the anatomical location of functionally active sites through comparison with functional maps.

For functional imaging studies, a single-shot blipped EPI technique with a matrix size of 64 × 64 pixels was used. Each image with a bandwidth of 200 kHz was acquired in 30 ms. Typical imaging parameters were a TE of 25 ms, a FOV of 24 × 24 cm^2, and a slice thickness of 10 mm.

As mentioned above, two temporal fMRI experiments were performed; one involves an immediate response ("Experiment I"), and the other one a delayed response ("Experiment II"). In Experiment I, we determined temporal resolution and reproducibility in *one single* area. The task consisted of a visually instructed four-digit movement in random order. Four circles, one for each finger, were used for the instruction. Whenever a circle was lit, the subject moved the corresponding finger. The order of fingers to move in each sequence was randomized between sequences to minimize motor learning components. The delay time between the end of one four-finger sequence and the beginning of the next four-finger sequence was randomized between 1 and 9.5 s. A reaction time was obtained from the average of the intervals between visual instruction and motor execution for the four movements within a four-finger sequence. The behavioral inter-epoch time was defined as the interval between onsets of consecutive sequences of four-finger movements, and measured through a pressure sensor attached to the keypad. Each experiment consisted of alternating control and task periods, with 8 to 12 sequences of movements during each task period. During the control period, the screen was dark. Typically, 60–80 images were acquired in each period. TR was 0.87 s (with three slices per image), and the flip angle was 45°.

Experiment II served to simultaneously determine hemodynamic responses in *multiple regions* during visually instructed, *delayed* four-digit movements in random order (Fig. 1). A row of four circles, one for each finger, was used for an instruction, as in Experiment I. A fifth circle at the top of the screen was used as a GO instruction. Each experiment consisted of three different periods. The first period was the presentation period: the

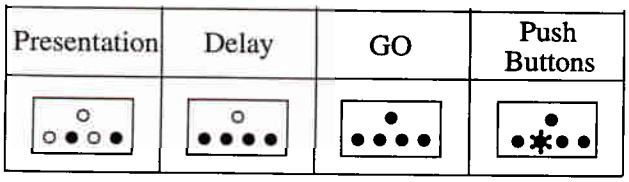

FIG. 1. Visually instructed, delayed motor task for Experiment II.

circles, initially empty, were sequentially filled with a color, one every 700 ms, yielding a total presentation time of 2.1 s. The order of the filled circles defined the order of finger movements. The second period was a delay time, which was varied between 0 and 7.0 s. During this period, the four circles remained filled while the subject was presumably mentally preparing the finger movement. The last period was the execution period; after the GO circle was lit, the subject pressed the buttons in the prescribed order; when each button was pressed, the corresponding circle blinked once. Hence, this experiment consisted of only one task period, surrounded by two control periods, with a single four-finger movement sequence during the task period. *TR* was 197 ms (with three slices), and the flip angle was 31° (the Ernst angle).

Functional MRI data were processed by using the software STIMULATE (developed in this laboratory). Areas of functional activation in both experiments were determined by using data from Experiment I; functional activation maps were calculated by a cross-correlation method with a boxcar reference function on a pixel-by-pixel basis (11). Since signal-to-noise ratios and activation intensities may vary among subjects, the correlation thresholds were individually adjusted to localize the activated areas; typically, the cross-correlation threshold was 0.4. An important issue is the significance of spatial variations of task-induced hemodynamic response times. To examine this question, a time course obtained from the pixels in motor areas which are active according to the above-mentioned criteria was used as a reference function. This reference function was shifted in time until maximal cross-correlation with the actual time course for each pixel was obtained.

From the anatomic images and the functional maps, the regions of interest (e.g., contralateral motor cortex and bilateral associative visual areas) were identified. Time courses were obtained from the pixels activated during the steady state condition within the region of interest, and smoothed by binominally weighted three-point averaging. Peaks were defined as maxima in fMRI time courses. The hemodynamic response time, defined as the interval between the temporal center of each four-finger movement and the corresponding fMRI peak was calculated. Only resolved peaks were included.

RESULTS

Figure 2 shows the result of Experiment I for one subject during right hand finger movements. Shown are a representative functional map, including the time shift of the hemodynamic response as determined by cross correlation (see Methods section) (Fig. 2A), the pressure curve detecting finger movements (Fig. 2B), and the fMRI time

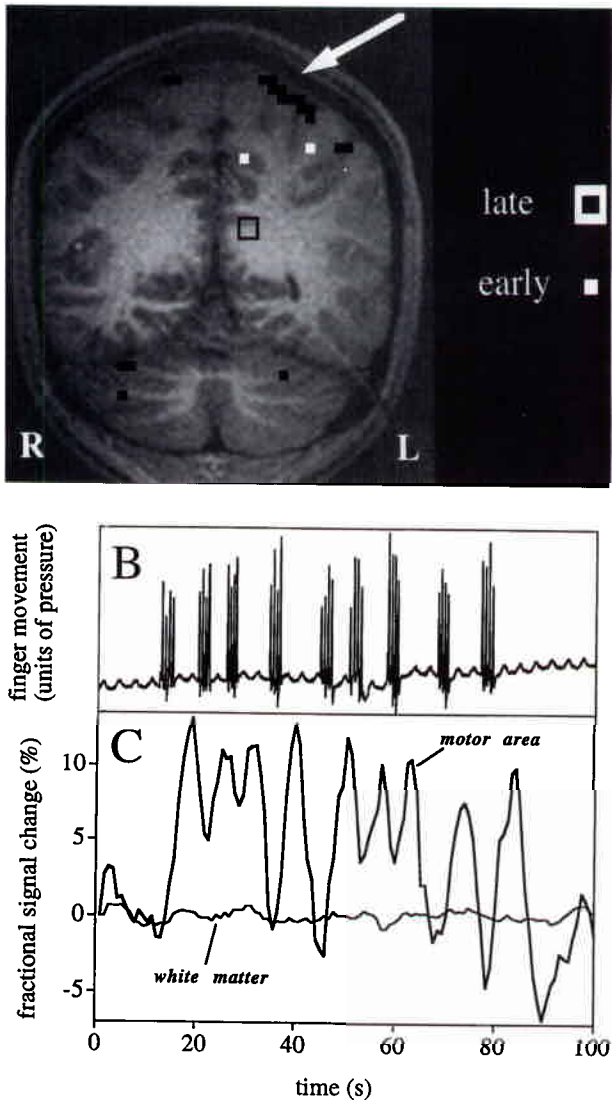

FIG. 2. A typical functional map overlaid on a T_1-weighted image (A), and pressure sensor and fMRI time courses (B and C). The black and white represent response times, as determined by time-shifted cross-correlation; the white pixels show maximal correlation less than one image (0.87 s) before the black pixels. The arrow indicates the left motor area and the box represents a white matter area, both giving rise to the time courses in C. R and L denote right and left hemisphere, respectively.

courses of pixels in the left (contralateral) motor cortex and white matter (Fig. 2C). The delay time between the end of the execution of a four-finger sequence and the start of the next four-finger sequence was between 3 and 7.5 s, and the time between onsets of subsequent tasks was about 5–9.5 s. During right hand finger movements, localized activation was seen predominantly in the left motor area (shown by the arrow), consistent with previous observations (22, 23). The hemodynamic response time difference between activated pixels is less than one image (0.87 s) and may be due to noise. Hence, time courses were obtained by averaging all active pixels within the motor area (Fig. 2A). Careful inspection of pressure data (Fig. 2B) shows that breathing appears as a

modulation of approximately 0.3 Hz because the pressure sensor was positioned on the abdomen; this observation was confirmed by monitoring the breathing rate independently. The large peaks in the pressure time course correspond to finger movements. The peaks in the fMRI signal time course of the motor cortex are well separated and closely correlated to the finger movements, while no significant signal change was observed in a white matter area (Fig. 2C). The fMRI signal peaks in the motor area were shifted from the task execution time by about 4.8 s. This hemodynamic response time was found to be constant during the experiment.

In all eight subjects, localized contralateral motor cortical activation was observed, and the correlation between fMRI time course in the motor area and finger movements was excellent. Figure 3 shows the hemodynamic response times (dotted bars) and average reaction times (filled circles) for the individual subjects. Means and standard deviations were calculated from repeated episodes of four-finger movement sequences with different inter-sequence delays. The hemodynamic response time varied between 3.7 and 6.8 s, and the average reaction times ranged from 400 to 670 ms. Only a weak correlation of the hemodynamic response time with the reaction time was observed (correlation coefficient = 0.63, R^2 = 0.39).

To determine the upper limit of temporal resolution in the motor area during repeated tasks, the inter-peak time in the fMRI data is plotted against the inter-epoch time (Fig. 4). Only resolvable fMRI signal peaks were included; for inter-epoch times of less than about 4 s, the corresponding fMRI signal peaks could not be resolved. The correlation between inter-peak interval and inter-epoch time is excellent (R^2 = 0.89). The *y* intercept is close to 0, as expected. The slope of this line is close to 1, and its standard deviation is 0.9 s. The latter is approximately equal to the *TR* of the fMRI data (i.e., 0.87 s per image); however, it may, in principle, be improved by using a higher sampling rate and, if necessary, temporal interpolation. In any case, the temporal resolution in this experiment cannot be better than the sampling rate if no assumptions to the response function are made.

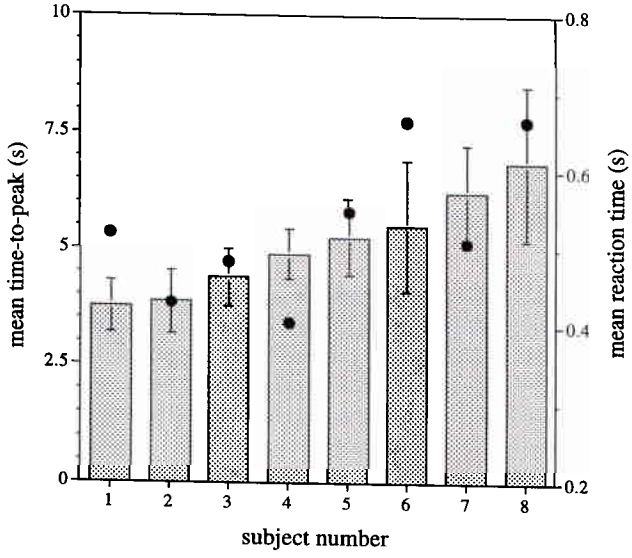

FIG. 3. Hemodynamic response time (dotted bars) and average reaction time (filled circles) of individual subjects during visually instructed four-finger movements. Error bars indicate standard deviations of hemodynamic response times.

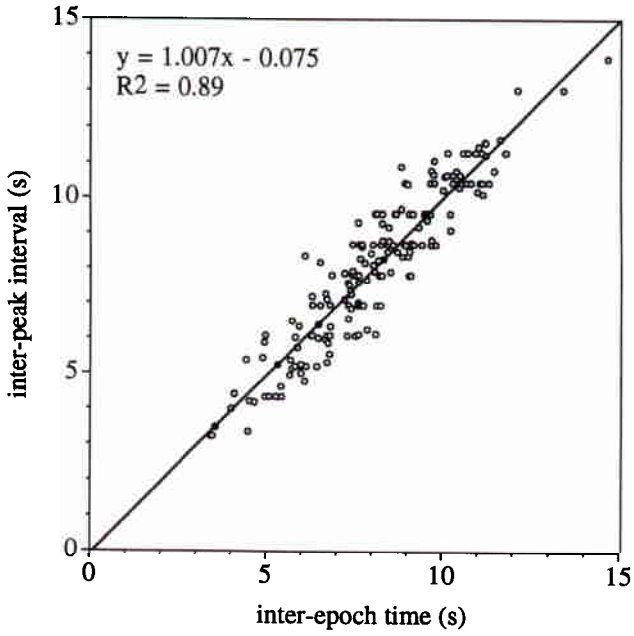

FIG. 4. Correlation between inter-fMRI signal peak interval and inter-epoch time. The open circles indicate actual data, and the solid line is a linear fit.

A higher temporal resolution can in principle be obtained among two spatially different areas such as motor and visual cortices. Figure 5 shows the results of Experiment II, with four delay times: 0, 2, 4, and 7 s. Time courses were extracted from the bilateral associative visual areas and the contralateral motor area (shown in Fig. 2A). After the presentation of the task, the fMRI signal increases in the bilateral visual areas and remains high for the rest of the task period in all four experiments. During the delay time, the subjects presumably prepared the movement; after the visual GO cue, the subjects moved their fingers, which was confirmed by the pressure data. After the motor execution, a signal increase in the motor cortex can be seen clearly. In several subjects, small signal changes in the motor cortex were observed during the motor preparation time (4 and 7 s) before the GO cue even though the corresponding pressure data suggested that finger movements were absent during that time. Differences of initial hemodynamic responses of both motor (variable) and visual (fixed) area agree extremely well with delay times. Although quantification is difficult because of the presence of activation in the motor cortex during the delay period, we estimate that delay time differences of 1–2 s can be resolved.

DISCUSSION

In this study, at high magnetic field and with the high temporal resolution provided by the EPI technique, *a single sequence of four finger movements* can be detected

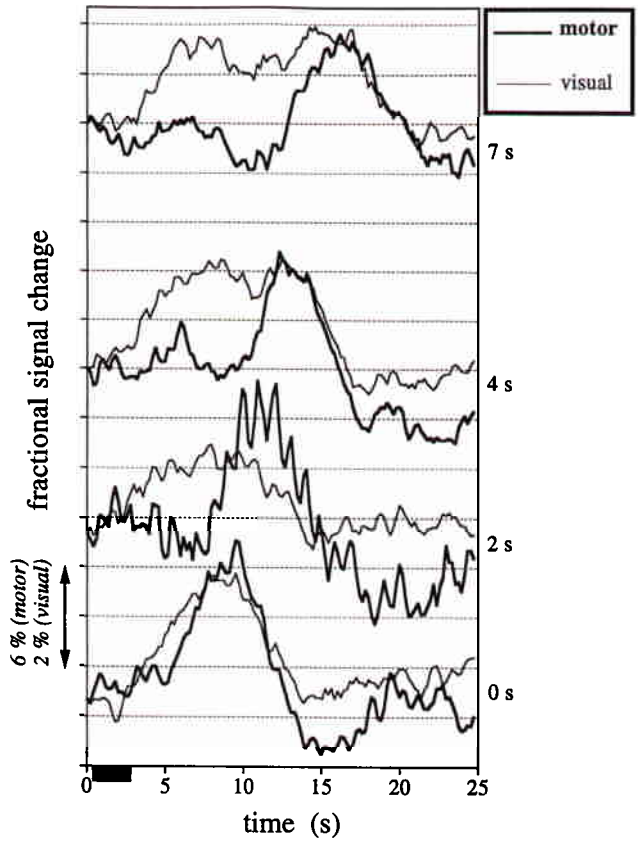

FIG. 5. Time courses of visual (thin line) and motor (thick line) areas during visually instructed, delayed motor tasks with delay times of 0, 2, 4, and 7 s, respectively. The filled box represents the duration of the visual presentation for a movement sequence (2.1 s). *TR* is 197 ms.

by fMRI without averaging. The upper limit of temporal resolution of hemodynamic response in the motor area during repeated tasks was approximately 5 s. The temporal resolution may be further increased by averaging fMRI time courses of the same subject to obtain higher SNR, and by mathematical deconvolution of fMRI peaks provided that the response function is linear (24). Averaging of time courses, however, must be performed by using actual behavioral data, such as finger movement times, as a time-lock reference. Whenever the reaction time varies considerably from one task to the next, as commonly seen in cognitive tasks, the fMRI time courses cannot easily be averaged.

Recently, negative BOLD signal changes within 2–3 s following visual stimulation have been observed (25). Even at 4 T with a surface coil, data from many trials were averaged to obtain this initial negative change. In our study, we did not detect initial negative signal changes in the primary motor and associative visual areas for two reasons. (i) The SNR of the data is poor because a homogeneous coil was used and no signal averaging was performed. (ii) The associate visual area was studied, rather than the primary visual cortex, in which the initial negative change has been observed.

The *average* hemodynamic response time of several trials can be determined by a shifted cross-correlation method (11); to use this method accurately, each task must be synchronized with the image collection. In our study, the presentation of all tasks but the first one, and the subsequent finger movements were not synchronized with the image collection. Thus, the hemodynamic response time was determined individually for each trial; then mean and variation were calculated.

Spatial distribution of hemodynamic response times may provide information about activation sites. Lee *et al.* (15) studied the hemodynamic response time during photic stimulation; the hemodynamic response times of gray matter and large vessel areas were 4–8 and 8–14 s, respectively. Hemodynamic response times reported here are less than 8 s, and the variability in hemodynamic response times in each subject was approximately 0.87 s, corresponding to the *TR* of the fMRI data collection. This suggests that the activated pixels *are not located at large vessels.* Also, since stimulation periods are shorter (approximately 2 s) than those of Lee *et al.* (15), smaller temporal variations are observed.

The hemodynamic response time in the motor cortex was constant for repeated tasks *in a single imaging session for a single subject* but varied among subjects; furthermore, the correlation between hemodynamic response time and reaction time was only weak. This observation suggests that the differences in hemodynamic response are related to different vascular architecture and/or other physiological parameters that regulate rCBF (15). Another implication of these results is that different parts of the brain of *a single subject* may have different hemodynamic response times due to different vascular environments; this point remains to be experimentally examined.

In principle, temporal resolution is better when the temporal evolution of spatially distinct regions is examined. The slow hemodynamic response introduces a "filter" that disperses and delays the fMRI response to neuronal activity. If sequential neuronal events occur in the same region, separated by a time less than the temporal resolution (i.e., 4 s in the motor area), they cannot be registered as two events by the fMRI signal, unless deconvolution methods are applied that make additional assumptions to the hemodynamic response function. If the sites of interest are spatially distinct, however, the response of each region can be separately monitored, giving an additional degree of temporal resolution. To evaluate this possibility, temporal studies were performed during visually instructed, delayed, cued finger movements using variable delay times. By comparing time courses of visual and motor areas, it was possible to detect delay time variations of as little as 2 s. This can be further improved by signal averaging. It should be noted that serial neural processing with delay times of $\leq$100 ms can be measured by methods using electric or magnetic activity, but not by fMRI.

The afore-described temporal study also addressed another critical issue; namely, if a temporal difference is observed in the fMRI responses of two distinct regions in the brain, it may represent either temporal differences of neuronal activity, or simply differences in the hemodynamic response characteristics of the two regions. In this study, a well-defined, independently determined, vari-

able delay is introduced between the visual and primary motor activity. By correlating the difference of fMRI time courses in the two regions with the variable delay, the component only due to temporal differences in neuronal activity can be obtained because hemodynamic response times are subtracted out. The intercept of the correlation curve indicates differences between the hemodynamic response times in the two regions. Hence sequential neural activation can be observed during a single visuomotor task. It is recognized that the plethora of neural processes that operate in a domain of tens of milliseconds will remain beyond the capabilities of present fMRI techniques; these serial neural processes can be investigated by MEG and EEG. However, many behavioral tasks such as mental rotation (26) involve mental processes lasting from hundreds of milliseconds to several seconds. In this case, the processing sequence may be resolved by comparing fMRI responses corresponding to variable reaction times (e.g., different rotation angles in mental rotation tasks).

Note Added in Proof: Recently, we applied fMRI to study activation during different processing stages of a delayed task (Experiment II) in a single trial for a single subject, and found that the human primary motor, the premotor, and the supplementary motor areas are active during both movement preparation (Delay on Fig. 1) and movement execution (27).

ACKNOWLEDGMENTS

The authors thank John Strupp for his data processing software (STIMULATE) and Peter Andersen and Gregor Adriany for hardware support.

REFERENCES

1. M. E. Raichle, Circulatory and metabolic correlates of brain functional in normal humans, *in* "Handbook of Physiology - The Nervous System V," pp. 643–674, 1987.
2. M. F. Hartshorne, Single photon emission computed tomography, *in* "Functional Brain Imaging" (W. W. Orrison, J. D. Lewine, J. A. Sanders, M. F. Hartshorne, eds.), pp. 213–237, 1995.
3. S. Ogawa, D. W. Tank, R. S. Menon, J. M. Ellermann, S.-G. Kim, H. Merkle, K. Ugurbil, Intrinsic signal changes accompanying sensory stimulation: functional brain mapping using MRI. *Proc. Natl. Acad. Sci. USA* **89,** 5951–5955 (1992).
4. K. K. Kwong, J. W. Belliveau, D. A. Chesler, I. E. Goldberg, R. M. Weisskoff, B. P. Poncelet, D. N. Kennedy, B. E. Hoppel, M. S. Cohen, R. Turner, H.-M. Cheng, T. J. Brady, B. R. Rosen, Dynamic magnetic resonance imaging of human brain activity during primary sensory stimulation. *Proc. Natl. Acad. Sci. USA* **89,** 5675–5679 (1992).
5. P. A. Bandettini, E. C. Wong, R. S. Hinks, R. S. Tikofsky, J. S. Hyde, Time course EPI of human brain function during task activation. *Magn. Reson. Med.* **25,** 390–397 (1992).
6. C. S. Roy, C. S. Sherrington, On the regulation of blood supply of the brain. *J. Physiol.* **11,** 85–108 (1980).
7. H. H. Kornhuber, L. Deecke, Hirnpotentialländerungen bei Willkürbewegungen und passiven Bewegungen des Menschen: Bereitschaftspotential and reafferente potentiale. *Pfluegers Arch.* **284,** 1–17 (1965).
8. W. Lang, D. Cheyne, R. Kristeva, G. Beisteiner, L. Deecke, Three-dimensional localization of SMA activity preceding voluntary movement. *Exp. Brain Res.* **87,** 688–695 (1991).
9. P. Mansfield, Multi-planar image formation using NMR spin echoes. *J. Phys. C: Solid State Phys.* **10,** L 55 (1977).
10. S.-G. Kim, X. Hu, G. Adriany, K. Ugurbil, Fast interleaved echo-planar imaging with navigator: high resolution anatomic and functional images at 4 Tesla. *Magn. Reson. Med.* **35,** 895–902 (1996).
11. P. A. Bandettini, A. Jesmanowicz, E.C Wong, J. S. Hyde, Processing strategies for time-course data sets in functional MRI of the human brain. *Magn. Reson. Med.* **30,** 161–173 (1993).
12. S. Ogawa, R. S. Menon, D. Tank, S.-G. Kim, H. Merkle, J. M. Ellermann, K. Ugurbil, Functional brain mapping by blood oxygenation level-dependent contrast magnetic resonance imaging: a comparison of signal characteristics with a biophysical model. *Biophys. J.* **64,** 803–812 (1993).
13. R. Turner, P. Jezzard, H. Wen, K. K. Kwong, D. Le Bihan, T. Zeffiro, R. Balaban, Functional mapping of the human visual cortex at 4 and 1.5 Tesla using deoxygenation contrast EPI. *Magn. Reson. Med.* **29,** 277–279 (1993).
14. R. M. Weisskoff, C. S. Zuo, J. L. Boxerman, B. R. Rosen, Microscopic susceptibility variation and transverse relaxation: theory and experiment. *Magn. Reson. Med.* **31,** 601–610 (1994).
15. A. T. Lee, G. H. Glover, C. H. Meyer, Distribution of large venous vessels in time-course spiral blood-oxygen-level-dependent magnetic resonance functional neuroimaging. *Magn. Reson. Med.* **33,** 745–754 (1995).
16. R. L. Savoy, P. A. Bandettini, K. M. O'Craven, K. K. Kwong, T. L. Davis, J. R. Baker, J. W. Belliveau, R. M. Weisskoff, B. R. Rosen, Pushing the temporal resolution of fMRI: studies of very brief visual stimuli, onset variability and asynchrony, and stimulus-correlated changes in noise, *in* "Proc., SMR, 3rd Annual Meeting, 1995," p. 450.
17. J. Hykin, R. Coxon, R. Bowtell, P. Glover, P. Mansfield, Temporal differences in functional activation between separate regions of the brain investigation with single shot echo volumar imaging at 3.0 T, *in* "Proc., SMR, 3rd Annual Meeting, 1995," p. 451.
18. H. Mushiake, M. Inase, J. Tanji, Neural activity in the primate premotor, supplementary, and precentral motor cortex during visually guided and internally determined sequential movements. *J. Neurophysiol.* **66,** 705–718 (1991).
19. G. Adriany, J. T. Vaughan, P. Andersen, H. Merkle, M. Garwood, K. Ugurbil, Comparison between head volume coils at high fields, *in* "Proc., SMR, 3rd Annual Meeting, 1995," p. 747.
20. W. Chen, H. Merkle, P. Erhard, K. Ugurbil, A robust device for monitoring head movement during functional MRI studies, *in* "Proc., SMR, 3rd Annual Meeting, 1995," p. 747.
21. A. Haase, Snapshot FLASH MRI: Application to T1-, T2-, and chemical shift imaging. *Magn. Reson. Med.* **13,** 77–89 (1990).
22. S.-G. Kim, J. Ashe, A. Georgopoulos, H. Merkle, J. M. Ellermann, R. S. Menon, S. Ogawa, K. Ugurbil, Functional imaging of human motor cortex at high magnetic field. *J. Neurophyiol.* **69,** 297–302 (1993).
23. S.-G. Kim, J. Ashe, K. Hendrich, J. M. Ellermann, H. Merkle, K. Ugurbil, A. Georgopoulos, Functional magnetic resonance imaging of motor cortex: hemispheric asymmetry and handedness. *Science* **261,** 615–617 (1993).
24. J. Hykin, R. Bowtell, P. Glover, R. Coxon, L. D. Blumhardt, P. Mansfield, Investigation of the linearity of functional activation signal changes in the brain using echo planar imaging (EPI) at 3.0 T, *in* "Proc., SMR, 3rd Annual Meeting, 1995," p. 795.
25. R. S. Menon, S. Ogawa, J. S. Strupp, P. Andersen, K. Ugurbil, BOLD-based functional MRI at 4 Tesla includes a capillary bed contribution: echo-planar imaging correlates with previous optical imaging using intrinsic signals. *Magn. Reson. Med.* **33,** 453–459 (1995).
26. R. N. Shepard, J. Metzler, Mental rotation of three-dimensional objects. *Science* **171,** 701–703 (1973).
27. W. Richter, P. M. Andersen, A. P. Georgoplulos, S.-G. Kim, Sequential activity in human motor areas during a delayed cued finger movement task studied by time-resolved fMRI. *NeuroReport,* in press.